JOURNAL OF GUIDANCE, CONTROL, AND DYNAMICS
Vol. 32, No. 1, January–February 2009

Numerical Study of Optimal Trajectories with Singular Arcs for an Ariane 5 Launcher

P. Martinon*
Institut National de Recherche en Informatique et en Automatique, 78153 Rocquencourt Cedex, France
F. Bonnans†
Institut National de Recherche en Informatique et en Automatique, 78153 Rocquencourt Cedex, France
J. Laurent-Varin‡
Centre National d'Etudes Spatiales, 91023 Evry Cedex, France
and
E. Trélat§
Université d'Orléans, 45067 Orléans Cedex 2, France

DOI: 10.2514/1.37387

We study optimal trajectories with singular arcs, that is, flight phases with a nonmaximal thrust, for a space launcher problem. We consider a flight to the geostationary transfer orbit for a heavy multistage launcher (Ariane 5 class) and use a realistic physical model for the drag force and rocket thrust. For the preliminary results, we first solve the complete flight with stage separations, at full thrust. Then we focus on the first atmospheric climbing phase to investigate the possible existence of optimal trajectories with singular arcs. We primarily use an indirect shooting method based on Pontryagin's minimum principle, coupled with a continuation (homotopy) approach. Additional experiments are conducted using a basic direct method, which confirms the solutions obtained by the shooting. We study two slightly different launcher models and observe that modifying parameters such as the aerodynamic reference area and specific impulsion can indeed lead to optimal trajectories with either full thrust or singular arcs.

I. Introduction

WE CONSIDER a flight mission to the geostationary transfer orbit (GTO) for an Ariane 5 launcher, while maximizing the payload or, as a variant, minimizing the fuel consumption. We first solve the complete flight sequence up to the final orbit, assuming a maximal thrust for all propulsion systems. Then we focus on the atmospheric ascent phase, which has been studied, for instance, in [1–3]. We are more specifically interested in optimal trajectories with singular arcs (flight phases with a nonmaximal thrust) for the boosters. Because of the presence of tabulated data in the physical model, the exact expression of the singular control cannot be obtained from the time derivatives of the switching function. An alternate way to compute the singular control is provided, and numerical experiments are carried out for several launcher variants.

Received 3 March 2008; revision received 3 June 2008; accepted for publication 5 June 2008.

*Research Scientist, Team COMMANDS, Saclay and Centre de Mathématiques Appliquées, Ecole Polytechnique, 91128 Palaiseau; Pierre.Martinon@inria.fr.

†Senior Research Scientist, Team COMMANDS, Saclay and Centre de Mathématiques Appliquées, Ecole Polytechnique, 91128 Palaiseau; Frederic.Bonnans@inria.fr.

‡Engineer, Launchers Directorate, Rond-point de l'Espace, Evry; Julien.Laurent-Varin@cnes.fr.

§Professor, Laboratoire MAPMO, Unité Mixte de Recherche 6628 Centre National d'Etudes Spatiales, Fédération Denis Poisson, FR 2964, Bâtiment de Mathématiques BP 6759; Emmanuel.Trelat@univ-orleans.fr.

II. Problem Statement

A. State and Control Variables

The state variables include the position and speed of the launcher, in thee dimensions, as well as the masses of the three fuel-consuming parts of the launcher: m_1 for the two boosters (treated as one propulsion system), m_2 for the first stage, and m_3 for the second stage (m denoting the total mass). This allows us to treat the separations more easily, avoiding the discontinuities of the state variables. Such discontinuities can be treated properly when applying Pontryagin's minimum principle (see, for instance, [4]), but, in view of the disappointing numerical results, we get rid of the discontinuities by splitting the total mass. Because the original problem is with a free final time, we use the standard transformation to obtain a formulation with a fixed final time.

The control variables include the throttle $\alpha \in [0, 1]$ for the boosters (we assumed a maximal thrust for the propulsion systems of the stages) and the flight angles θ and ψ (heading and azimuth) that give the thrust direction. The control vector is then

$$u = (\alpha, \theta, \psi) \in [0, 1] \times [-\pi, \pi]^2 \tag{1}$$

B. Flight Dynamics

The dynamics for the masses correspond to the fuel consumption, which depends on the flight phase. The flight dynamics are

$$\begin{cases} \dot{r} = v \\ \dot{v} = (1/m)(T(r, u) - D(r, v)) + g(r) \\ \dot{m}_i = -\alpha\beta \quad \text{(for each fuel-consuming part)} \end{cases} \tag{2}$$

where $T(r, u) = \alpha\beta I_{sp} g_0 - SP_z$ is the rocket thrust, β is the mass flow rate, I_{sp} is the specific impulse, S is the area at the rocket exit, P_z is the atmospheric pressure (table), $D(r, v) = qSrC_x(M)$ is the drag due to the Earth's atmosphere, q is the dynamic pressure, S_r is the

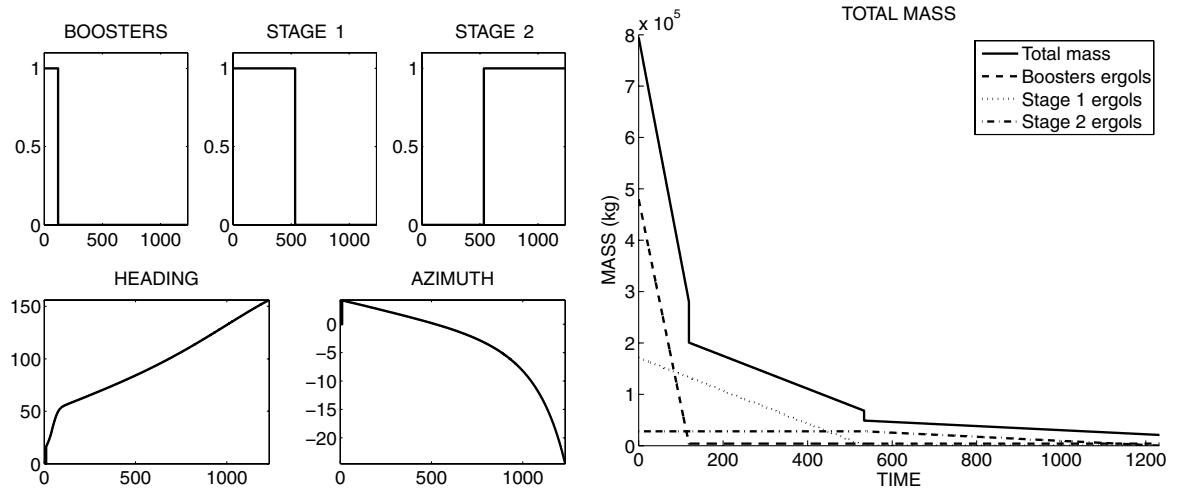

Fig. 1 Complete flight with full thrust: controls and masses.

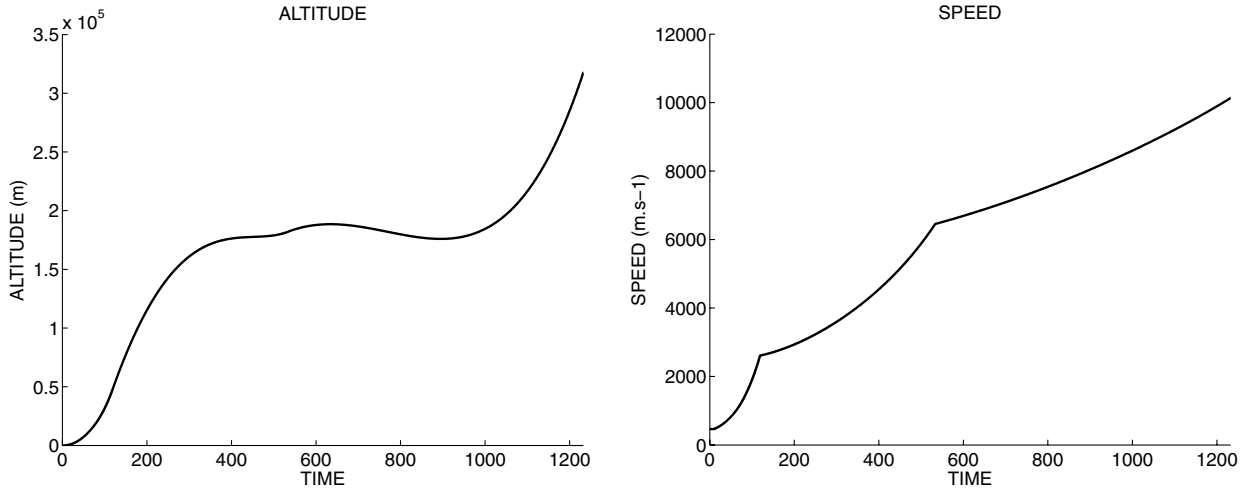

Fig. 2 Complete flight with full thrust: altitude and speed.

reference area, C_x is the drag coefficient (table), M is the speed in Mach, and $g(r) = -\frac{\mu}{\|r\|^3}(r + J_2 \frac{R_T^2}{\|r\|^2} M_{J_2} r)$ is the gravity with a J_2 corrector term. (Note: The lift term in the aerodynamic forces is omitted here.)

Applying Pontryagin's minimum principle shows a decoupling for the control variables. Minimizing the Hamiltonian leads to the thrust direction being opposite to the speed costate, whereas the throttle follows a bang–bang law, with possible switchings or singular arcs.

C. Complete Flight at Full Thrust

We start by solving the complete flight with stage separations by setting a full thrust for the boosters. Here, we want to maximize the payload and assume all fuel is burnt. As we consider the mass of each component instead of the global mass, the state variables remain continuous at the separation times. Therefore, the separation times t_1 and t_2 for the boosters and first stage only need to satisfy the continuity of the Hamiltonian. We introduce as additional shooting unknowns the value of the state and costate at the separation times, namely, (x^1, p^1) and (x^2, p^2), for a better numerical behavior. We have the corresponding matching conditions that enforce the continuity of x and p at the separation times.

D. Numerical Results

Solving the complete flight problem directly with the shooting method is difficult, due to the lack of a suitable initial guess. We first solve the flight restricted to the first phase (until separation of the boosters), then add the second and third phases. We obtain a solution with a payload of 14,623 kg and a final time of 1232.75 s. Booster separation occurs after 119 and 533.375 s for the first stage, which is consistent with the constraints set on the final masses (consumption of all fuel).

Remark: The thrust is actually completely fixed during the first 10 s of the flight, vertical and maximal.

The graphs in Fig. 1 represent the optimal control with the thrust level for the boosters and two stages, the heading and azimuth angles for the thrust direction, and the masses of the different parts of the launcher. The separations correspond to the discontinuities observed in the total mass.

Figure 2 shows the evolution of the altitude and speed of the launcher during the flight. The change of the propulsion system at the beginning of the second and third phases is clearly visible on the speed graph. These graphs are consistent with the typical GTO flight described, for instance, in the Ariane 5 user's manual from Arianespace.¶

Remark: It should be kept in mind that we have allowed a free direction for the thrust, which is not the case in the real flight in which the thrust direction is strongly constrained by the dynamic pressure limit. However, the trajectory we obtained is close to the reference one.

¶Data available online at http://www.arianespace.com/site/index.html [retrieved 1 August 2008].

III. Study of Singular Arcs for Boosters

We focus now on the study of singular arcs for the boosters, whose throttle is now free in [0, 1], while keeping a maximal thrust for the two stages. We also restrict the flight to the first atmospheric climbing phase until the separation of the boosters. We reformulate the payload maximization criterion into a fuel consumption minimization, which is more suitable for the study of singular arcs. As we are only considering a variable throttle for the boosters (the etage accélérateur à poudre, or EAP), we set as the new criterion

$$\text{Min} \int_0^{t_f} \alpha \beta_{\text{EAP}} \tag{3}$$

The payload is now fixed and is no longer part of the state variables, and the final masses m_1, m_2, m_3 are free. We also replace the final condition on the orbit with new final conditions on the position and speed. We take the values corresponding to the boosters' separation on the trajectory previously computed for the complete flight with full thrust.

A. Alternate Expression for Singular Control

A singular arc is characterized by the fact that the switching function ψ (the derivative of the Hamiltonian with respect to the control) vanishes over a whole time interval. The expression of the singular control is usually obtained by differentiating the equation $\psi(x, p) = 0$ with respect to time until the control appears explicitly (the required order of differentiation being always even; see, for instance, [5]). However, due to the presence of tabulated data in the thrust and drag terms, the analytic expression of $\ddot{\psi}$ is not already available. We only have the first derivative $\dot{\psi}$ that depends on $\dot{x}$ and $\dot{p}$. As the idea behind the formal expression of the singular control is that the switching function and its successive time derivatives vanish over a singular arc, we try to enforce this constraint with the terms at our disposal.

Therefore, for the singular control, we choose at each time step the value $\tilde{\alpha}_{\text{sing}}$ that minimizes ψ and $\dot{\psi}$ at the next integration step, that is,

$$\tilde{\alpha}_{\text{sing}} = \text{ArgMin}_{[0,1]} \|(\psi(y_{i+1}), \dot{\psi}(y_{i+1}))'\|^2 = \psi^2(y_{i+1}) + \dot{\psi}^2(y_{i+1}) \tag{4}$$

where y_{i+1} denotes the state–costate pair (x, p) obtained after one integration step from the current time. This minimization is currently performed by a Broyden–Fletcher–Goldfar–Shanno method [6], starting from an initial value $\alpha = 0.5$. The numerical experiments showed that taking 0.1 or 0.9 as the initial value gives similar results, which is, of course, reassuring. Furthermore, using the singular control continuity to initialize this minimization step (after the arc entry) seems to give slightly better results than using a constant initialization.

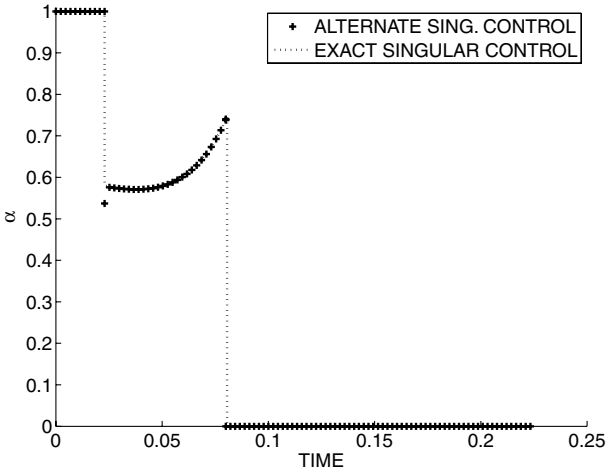

Fig. 3 Three-dimensional Goddard problem: approximate and exact singular control.

We tested this formulation on the three-dimensional Goddard problem (cf. [7]) and found control values quite close to the exact value of α^*_{sing} obtained from the equation $\ddot{\psi}(x, p) = 0$; see Fig. 3. The difference between the exact singular control and the alternate formulation is about 10^{-3}, but the computational cost increased significantly. However, the minimization procedure was not optimized and so might be further improved.

B. Continuation Approach for Singular Arcs

To solve a problem with singular arcs, in addition to the expression of the singular control, we also need some information about the control structure, namely, the number and position of the singular arcs. To obtain such information, we approach the original problem with a sequence of regularized problems with strictly convex Hamiltonians (with respect to the throttle), such as in [7,8], for instance. This is done by adding a quadratic term to the criterion, which becomes, for given $\lambda \in [0, 1]$,

$$\text{Min} \int_0^{t_f} [\alpha \beta_{\text{EAP}} + (1 - \lambda)\alpha^2 \beta_{\text{EAP}}]\, \text{d}t \tag{5}$$

This regularization adds a new term, $(1 - \lambda)\alpha^2 \beta_{\text{EAP}}$, to the Hamiltonian, which gives the modified command law for $\lambda < 1$:

$$\begin{cases} \text{If } \psi(x, p) > 0 & \text{then } \alpha = 0 \\ \text{If } \psi(x, p) < -2(1 - \lambda)\beta_{\text{EAP}} & \text{then } \alpha = 1 \\ \text{If } -2(1 - \lambda)\beta_{\text{EAP}} < \psi(x, p) < 0 & \text{then } \alpha = \frac{-\psi(x,p)}{2(1-\lambda)\beta_{\text{EAP}}} \end{cases} \tag{6}$$

The optimal control is now continuous, without singular arcs or switchings.

We perform a discrete continuation on this problem family and solve an automated sequence of problems $(P)_\lambda$ starting from $\lambda = 0$. We use a very basic algorithm to generate the sequence of problems:

1) Solve (P_0).

2) Iterate: set $\lambda_{k+1} = \lambda_k + h$ and solve $(P_{\lambda_{k+1}})$ using (P_{λ_k}) as the initialization with a linear prediction ($h = 1$ initially, and is decreased in case of failure).

3) Stop when $\lambda = 1$ is reached, or the maximum number of iterations/minimal step size for h.

Notice that we do not actually need to reach $\lambda = 1$, but we still need to obtain sufficient information regarding the control structure, as well as a suitable initialization for the shooting method adapted to the singular structure.

However, even the strongly regularized problem (P_0) is not easy to solve directly, and so we add a second layer of continuation over the atmospheric forces, gradually introducing the atmospheric drag for the problem (P_0). Numerical experiments indicate that it is usually easy to solve the regularized problem in a vacuum and complete the continuation on the drag, which gives a solution for the regularized problem (P_0). We can then begin the regularization homotopy to determine the control structure. The results of this method are described next, first for the original Ariane 5 launcher and then for a slightly modified launcher.

Note: All numerical simulations were run on a standard desktop computer (Pentium IV 2.4 GHz) using the GFORTRAN compiler. Using a fixed-step Runge–Kutta fourth-order (RK4) integration (100 steps) and the HYBRD solver (see [9]) for the shooting method, the total CPU time for the atmosphere and regularization continuations and the final shooting is about 10 min.

C. Study of Original Launcher

We first apply the approach already described to the original launcher problem, with a fixed payload $m_{\text{CU}} = 12,610$ kg. The regularized problem in vacuum can be solved from a very simple starting point: $(t_f = 100,\ p_r(0) = (-0.1, -0.1, 0.1),\ p_v(0) = (-10^3, -10^3, -10^3)$, and $p_i(0) = -0.1, i = 1 \cdots 3)$. The preliminary continuation is performed without any difficulties and gives a solution of (P_0). During the main continuation, we observe (in Fig. 4) that the interval with a nonmaximal thrust becomes smaller

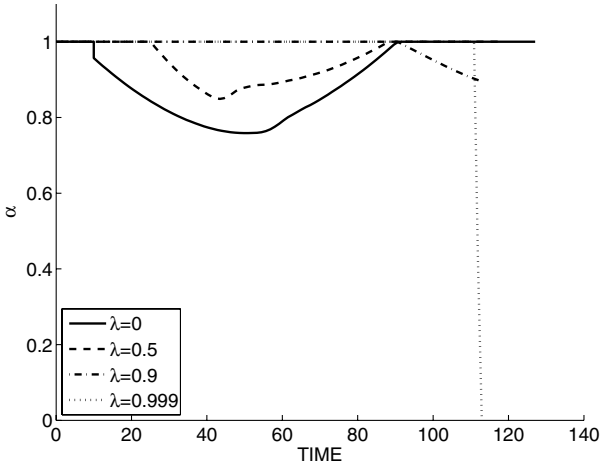

Fig. 4 Regularization homotopy: thrust level for $\lambda = 0$, 0.5, 0.9, and 0.999.

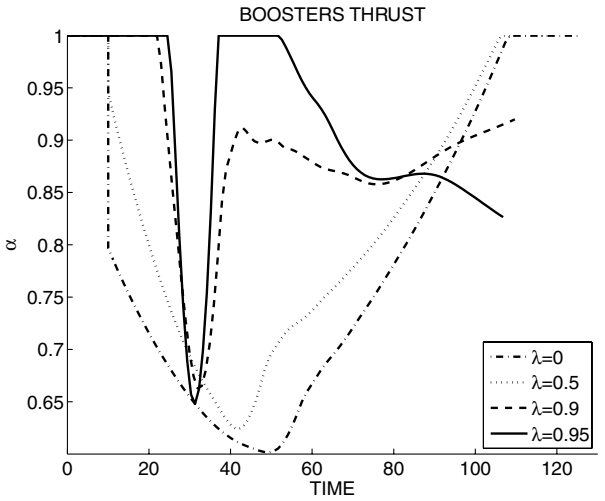

Fig. 5 Regularization homotopy: thrust level for $\lambda = 0$, 0.5, 0.9, and 0.95.

when the regularization decreases as λ tends to 1. At $\lambda = 0.999$, we have a solution with a full thrust throughout the flight except for the last few seconds, but with no sign of a singular arc.

We conduct some simple experiments with a direct method: a piecewise constant control with 100 steps, an RK4 integration for the state, and the IPOPT ([10]) solver for the resulting optimization problem. We find a similar solution, with a full thrust and a switching to null thrust just before the end of the flight. Thus, both methods suggest that the optimal solution to this problem does not present singular arcs.

D. Study of Modified Launcher

Now we modify the launcher parameters to increase the drag effect; we increase the reference area S_r and the specific impulse $I_{\mathrm{sp}_{\mathrm{EAP}}}$. For $S_r \times 2$ and $I_{\mathrm{sp}_{\mathrm{EAP}}} \times 1.25$, we find an optimal trajectory with a singular arc.

As before, the regularized problem with no drag is easily solved, and the first continuation to introduce the drag poses no difficulties. Then we perform the regularization continuation until $\lambda = 0.95$, which shows strong hints of a singular arc. The graphs in Fig. 5 show the thrust level and switching function at the solutions for $\lambda = 0$, 0.5, 0.9, and 0.95. Contrary to the previous case, we observe a small time interval (around $t = 30$ s) in which the thrust level remains in]0, 1[. Moreover, we see that the switching function ψ comes closer to 0 at the same time interval. These two facts together strongly suggest the presence of a singular arc. What happens at the end of the flight is less clear, as the thrust level again takes values in]0, 1[and decreases near

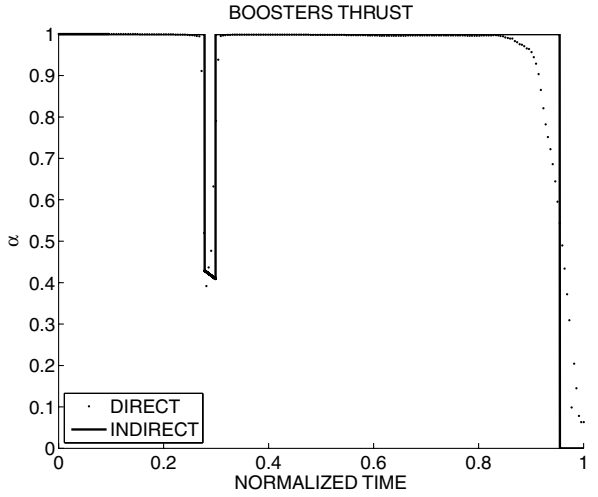

Fig. 6 Solution with a singular arc for $\lambda = 1$.

t_f. This could indicate a second singular arc, maybe followed by an arc with a null thrust or just a switching to a null thrust arc.

The shooting method fails to converge for structures with two singular arcs, but the formulation with one arc actually gives a solution with a singular arc and a switching at the end. We detail herein the shooting formulation for a control structure assuming one interior singular arc. In addition to the usual shooting unknowns (final time and initial costate), we have the entry and exit times for the singular arc. The corresponding additional conditions ensure that we enter the switching surface tangentially at t_{entry}, that is, $\psi(x(t_{\mathrm{entry}}), p(t_{\mathrm{entry}}) = \dot{\psi}(x(t_{\mathrm{entry}}), p(t_{\mathrm{entry}})) = 0$; see, for instance, [4]. Notice that the switching at the end is handled automatically by a switching detection algorithm checking the sign of the switching function during the integration (see, for instance, [11], pages 195–200).

Shooting formulation for one interior singular arc:

1) Shooting function unknown $z \in \mathbf{R}^{12}$: $z = (t_f, p_r(0), p_v(0), p_m(0), t_{\mathrm{entry}}, t_{\mathrm{exit}})$.

We use the solution from the end of the regularization continuation ($\lambda = 0.986$ after 100 iterations) to initialize z.

2) Shooting function value $S(z) \in \mathbf{R}^{12}$:

$$\begin{cases} r(t_f) - r_f & \text{final position} \\ v(t_f) - v_f & \text{final speed} \\ p_{t_f}(t_f) & \text{final time TC} \\ p_{m_i}(t_f), i = 1 \cdots 3 & \text{final masses TC} \\ \psi(x(t_{\mathrm{entry}}),\ p(t_{\mathrm{entry}})) & \text{switching conditions} \\ \dot{\psi}(x(t_{\mathrm{entry}}),\ p(t_{\mathrm{entry}})) & \text{at entry time} \end{cases} \tag{7}$$

where TC is defined as the transversality conditions.

Once again, we test a basic direct method and find a similar solution. The graph in Fig. 6 shows these results, with the small singular arc (about 2 s) clearly visible in both solutions from the indirect and direct methods, around $t = 30$ s. Both solutions also confirm that we have a simple switching near the end of the flight, and not a second singular arc.

As expected, the switching function ψ and its first derivative $\dot{\psi}$ are both close to 0 on the singular arc, around 10^{-3} and 10^{-4},

Table 1 Singular arc duration and mass gain for increasing S_r

	$S_r \times 2$	$S_r \times 2.5$	$S_r \times 3$
$m_1(t_f)$ (singular arc), kg	165,163	160,199	155,986
$m_1(t_f)$ (bang–bang), kg	164,442	159,172	154,202
Arc duration, s	2.1	——	15.3
Mass gain, kg	721	1027	1784

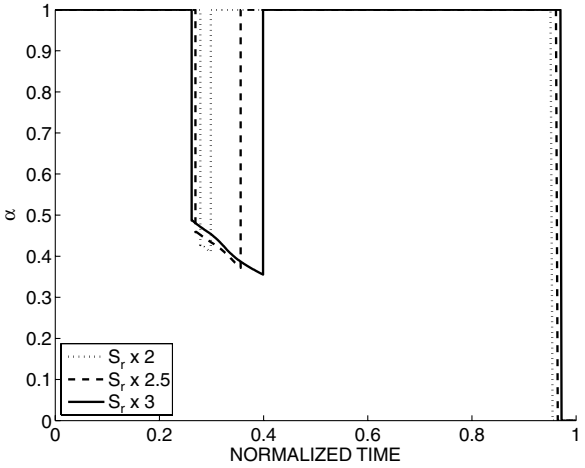

Fig. 7 Singular arcs for increasing values of S_r.

respectively. Thus, the approach of computing the singular control that minimizes $\psi^2 + \dot{\psi}^2$ worked rather well on this problem.

The criterion value (i.e., the final mass of the EAP) is quite close for both solutions, with $m_1(t_f) = 165,163$ kg for the shooting method and $m_1(t_f) = 164,990$ kg for the direct method. Solving the same problem with the direct method with a fixed bang(1)–bang(0) control structure gives a close solution (without the singular arc, of course), with a criterion of $m_1(t_f) = 164,442$ kg. It is comforting to observe that the solution with the singular arc is indeed slightly better than the forced bang–bang one, even if the difference is quite small.

It seems reasonable to assume that, for a different set of parameters that would give a solution with a longer singular arc, the gain compared with the bang–bang solution would be more significant. Indeed, we can perform a continuation directly on the solution with a singular arc and further increase the value of the parameter S_r. We observe that the solutions exhibit longer singular arcs when S_r increases, with a more significant gain with respect to the corresponding solution (Table 1 and Fig. 7).

IV. Conclusions

This study indicates that, although the original problem for an Ariane 5 launcher seems to have a simple bang–bang optimal solution, slightly modifying some parameters such as the reference area and specific impulse of the launcher gives an optimal solution with a singular arc. We also introduced a new way of computing the singular control when its analytic expression from the time derivatives of the switching function is not available (due here to the presence of tabulated data in the physical model). We plan to extend this work to the study of a winged launcher while taking into account the lift force and dynamic pressure constraint.

Acknowledgement

This study was supported by the Centre National d'Etudes Spatiales, Paris.

References

[1] Seywald, H., and Cliff, E. M., "Goddard Problem in Presence of a Dynamic Pressure Limit," *Journal of Guidance, Control, and Dynamics*, Vol. 16, No. 4, 1993, pp. 776–781. doi:10.2514/3.21080

[2] Calise, A. J., and Gath, P. F., "Optimization of Launch Vehicle Ascent Trajectories with Path Constraints and Coast Arcs," *Journal of Guidance, Control, and Dynamics*, Vol. 24, No. 2, 2001, pp. 296–304.

[3] Lu, P., Sun, H., and Tsai, B., "Closed-Loop Endoatmospheric Ascent Guidance," *Journal of Guidance, Control, and Dynamics*, Vol. 26, No. 2, 2003, pp. 283–294.

[4] Pesch, H. J., "A Practical Guide to the Solution of Real-Life Optimal Control Problems," *Control and Cybernetics*, Vol. 23, Nos. 1–2, 1994, pp. 7–60.

[5] Robbins, H. M., "A Generalized Legendre-Clebsch Condition for the Singular Case of Optimal Control," *IBM Journal of Research and Development*, Vol. 11, July 1967, pp. 361–372.

[6] Byrd, R. H., Lu, P., Nocedal, J., and Zhu, C. Y., "A Limited Memory Algorithm for Bound Constrained Optimization," *SIAM Journal on Scientific Computing*, Vol. 16, No. 5, 1995, pp. 1190–1208. doi:10.1137/0916069

[7] Bonnans, F., Martinon, P., and Tŕelat, E., "Singular Arcs in the Generalized Goddard's Problem," *Journal of Optimization Theory and Applications*, Vol. 138, No. 2, Aug. 2008. doi:10.1007/s10957-008-9387-1

[8] Gergaud, J., and Martinon, P., "An Application of PL Continuation Methods to Singular Arcs Problems," *Recent Advances in Optimization*, edited by A. Seeger, Vol. 563, Lectures Notes in Economics and Mathematical Systems,Springer–Verlag, Berlin/New York/Heidelberg, 2006, pp. 163–186.

[9] Garbow, B. S., Hillstrom, K. E., and More, J. J., *User Guide for Minpack-1*, Argonne National Laboratory, Chicago, 1980.

[10] Waechter, A., and Biegler, L. T., "On the Implementation of an Interior-Point Filter Line-Search Algorithm for Large-Scale Nonlinear Programming," *Mathematical Programming, Series A*, Vol. 106, No. 1, March 2006, pp. 25–57. doi:10.1007/s10107-004-0559-y

[11] Hairer, E., Nørsett, S. P., and Wanner, G., "Dense Output, Discontinuities, Derivatives," *Solving Ordinary Differential Equations I*, Vol. 8, Springer Series in Computational Mathematics, Springer–Verlag, Berlin, 1993, pp. 195–200.